Hydrogeologic and Geochemical Distinctions in Freshwater-Brine Systems of an Andean Salar

L. A. Munk[1] 0000-0003-2850-545X, D. F. Boutt[2] 0000-0003-1397-0279, B. J. Moran[2] 0000-0002-9862-6241, S. V. McKnight[2] 0000-0002-6013-193X, J. Jenckes[1] 0000-0002-1811-3076

[1]Department of Geological Sciences, University of Alaska Anchorage

[2]Department of Geosciences, University of Massachusetts Amherst

Corresponding author: Lee Ann Munk (lamunk@alaska.edu)

Key Points:

- Distinct hydrogeologic and geochemical zones are inherent in salar freshwater-brine systems.
- Lagoons in the Transition Zone are perched by complex subsurface geology, depend on inflow waters, and respond to climate over time.
- Transition zone brines are geochemically distinct from nucleus brines and are hosted by a more geologically diverse aquifer system.

This article has been accepted for publication and undergone full peer review but has not been through the copyediting, typesetting, pagination and proofreading process, which may lead to differences between this version and the Version of Record. Please cite this article as doi: 10.1029/2020GC009345.

Abstract

The Salar de Atacama contains one of the world's most important lithium resources and hosts unique and fragile desert ecosystems. Water use issues of the hyper-arid region have placed it at the center of global attention. This work combines geochemical and hydrogeologic data with remote sensing analysis to address differences in water zones in the marginal environments of the salar. Water samples from across the inflow to brine transition were collected over the period 2012-2016 and analyzed for δD, ^{3}H, $^{87}Sr/^{86}Sr$ and major and minor elements. The δD values range from about -64 to +20 ‰, ^{3}H as R_{mod} from 0.01 to 0.36 and the $^{87}Sr/^{86}Sr$ from 0.70750 to 0.70804 with highest δD and ^{3}H occurring in the regions of open water. Geochemical modeling results indicate inflow and shallow transition zone waters are saturated with respect to calcite, whereas all others are saturated with respect to calcite, gypsum, and halite. Long-term remote-sensing of surface water body extents indicate that extreme precipitation events are the primary driver of surface area changes as exemplified by an increase in size of the lagoons by a factor of 2.7 after a storm. A new conceptual model of the freshwater to brine transition zone that incorporates variability in aquifer geology, hydrology and geochemistry to explain important marginal water bodies is presented. The subsurface brines in the transition zone and the halite nucleus are geochemically distinct compared to the groundwater discharge features (e.g. lagoons) over modern time scales which aids in conceptualizing the transition zone system.

Plain Language Summary

Salar (salt flat or playa) systems are of intense global focus because of associated water and resource issues. The freshwater-brine systems that are unique to these areas support important ecosystems as well as both resource development and community needs. This study includes a novel integrated analysis to demonstrate how the water bodies in the marginal zones of salars are controlled by the amount of fresh water flowing from higher elevation below the ground surface, the properties of the complex subsurface geology, and climate variability. The focus is on how freshwater recharge influences physical and chemical properties of marginal water bodies including springs, wetlands, lagoons, and transitional pools. Additionally, the two types of brines found in the marginal zone and from the center of the Salar de Atacama are distinct and evidently disconnected from the shallow groundwater discharge features. The methods and approach from this work are transferrable to salar systems on a global scale and can be used by

multiple stakeholders for decision making regarding resources and environment where an understanding of these water bodies is needed in assessing local and regional water use.

1 Introduction

The marginal environments of salar (e.g. salt flats) systems are unique ecological and hydrogeological regions of great importance in arid to hyper-arid climates (Rosen, 1994; Pigati et al., 2014: Warren, 2016). These distinctive places have become one of the most significant areas of concern in regions where groundwater and/or brine extraction are relied on for human use including resource development and fresh water sources used by communities (Tyler et al., 2006; Warren, 2010; Houston at al., 2011). As demand for water sources continues to increase (Wang et al., 2018; Zipper et al., 2020; Gleeson et al., 2020) it is critical to have a complete and scientifically based assessment of these transitional zone regions where freshwater discharges and evaporates above brackish and brine water in the subsurface. This process is what supports the formation of springs, wetlands or marshes (vegas), and lagoons (lagunas) that form important ecosystems on the margins of all salars on a global scale. However, the extent of development of these groundwater discharge features is unique among each salar which is reflective of the morphology, geology, elevation, and hydrology of each basin.

The work presented here builds on decades of research on salars, including the geochemical evolution of inflow waters to brines (e.g. Hardie and Eugster, 1970; Nesbitt, 1974; Eugster and Hardie, 1978), the geochemical and/or isotopic investigations specifically for South American salars (e.g. Moraga et al., 1974; Rettig et al., 1980; Risacher and Fritz, 2009; Alpers and Whitmore, 1990; Spiro and Chong, 1996; Carmona et al., 2000; Boschetti et al., 2007; Munk et al., 2018; Godfrey and Amado-Alvarez, 2020), the sedimentology and stratigraphy of closed-basin continental salars (e.g. Hardie et al., 1978; Smoot and Lowenstein (and refs. therein) 1991; Benison and Goldstein, 2001; Warren (and refs. therein) 2006;) and the importance of hydrology and stratigraphy of playas (Rosen, 1994). We provide a new paired geological, geochemical, and hydrological approach to investigating the transition zone region which is the link between freshwater and brine in these systems. Although the work presented is focused on a data-rich zone of the southern region of the Salar de Atacama (SdA), the methods, conceptual model, and

functioning of these systems is translational to other salars on a global basis. Each transition zone may have a unique set of groundwater discharge features and the morphology of those features may vary, even as they do at the SdA, but the combined hydrogeologic and geochemical processes that cause their formation are similar across salar systems. Therefore, our approach and methods may be used as a basic framework for investigating salars in other regions from a hydrogeochemical and geological standpoint.

This paper is focused on a detailed hydrogeochemical and physical investigation through one of the major lagoon systems at SdA which is based on a detailed sampling of a flow path of the shallow groundwater system and persistent surface water bodies (Figures 1 and 2). A new conceptual model of the zones of the upper fresh/brackish regime and the lower brine regime are developed based on the hydrogeochemistry, subsurface geology, and hydrologic properties. This work also contributes a new detailed investigation describing how the transition zones and their water features lack connection to the halite nucleus based on geochemical and hydrogeologic observations. These findings have fundamental implications for both environmental and resource issues surrounding these vital Li resources on a global scale.

2 Geologic and Hydrogeologic Setting of the Salar and Transition Zone

2.1 Regional Salar de Atacama Geology and Hydrogeology

The SdA is a significant topographic depression located within the volcanic arc of the Central Andes of Chile (Reutter et al, 2006). The salar at the basin floor covers 3,000 km^2 at an elevation of 2,300 m and is closed to the north, south and east by the Andean Cordillera (>5,500 m) and the Cordillera de Domeyko (>3,500 m) to the west. The rim of high volcanic peaks to the east and southeast delineates the SdA topographic watershed, encompassing over 17,000 km^2, and the western margin of the Altiplano-Puna Plateau (Allmendinger et al., 1997; Jordan et al, 2010). This vast, internally drained plateau ranging in elevation from 4,000 m to 6,000 m is underlain by the Altiplano-Puna Volcanic Complex (APVC) (de Silva, 1989; de Silva, 1989a); a succession of volcanic units deposited over the last 10 Ma by caldera forming eruptions which produced over 15,000 km^3 of dense-rock equivalent ignimbrites, small volume mafic centers and

numerous stratovolcanoes (Strecker et al., 2007; Ward et al., 2014). The volcanic complex and eastern slope of the basin is primarily composed of andesitic, rhyolitic, dacitic, and some basaltic volcanic rocks with alluvial, fluvial, and aeolian sediments and sedimentary rocks of primarily re-worked volcanic material (Schmitt, 2001; WMC, 2007). The stratovolcanoes including the high peaks on the topographic divide and possibly those buried under younger volcanic deposits are generally of high permeability (Gardeweg & Ramirez, 1987; WMC, 2007). The regionally extensive, voluminous ignimbrites are characterized by a remarkably homogenous composition that is predominantly calcalkaline dacite (Schmitt, 2001; Ward et al., 2014).

Miocene ignimbrite units draped across the region and alluvial fans along the flanks of the SdA basin appear to be important for transporting fluid to the springs emerging from the slopes and margins of the salar (Jordan et al., 2002; Mather & Hartley, 2005). The thick ignimbrite sequences and other volcanic rocks that occur within the SdA and blanket the surrounding high elevation areas, specifically the modern units (<5 Ma) are characterized by both welded and unwelded layers of varying thicknesses and extent (Houston & Hart, 2004). The unwelded ignimbrite sheets have high infiltration capacity and permeability, and they likely constitute the major flow paths of local and regional groundwater; the welded ignimbrites and other sequences of low hydraulic conductivity may act as important confining units (Houston, 2009; Herrera et al., 2016). Large accumulations of sedimentary and conglomerate sequences and buried alluvial fans such as those near the topographic divide could provide conduits for deep groundwater transport to the eastern slope (Wilson & Guan, 2004; Houston, 2009). Vertical leakage through fractured volcanic material and across stratigraphy may constitute flow paths with longer residence times.

The southeastern slope of SdA south of the Tumisa volcano is bounded to the southwest by the Monturaqui–Negrillar–Tilopozo (MNT) trough, a 60 km long N–S oriented depression. The Miscanti fault and fold to the east separates the basin from the Andes and controls the development of the intra-arc lakes Miñiques and Miscanti (Rissmann et al., 2015; Aron et al., 2008). A large lithospheric block of Paleozoic rock, bounded by the N-S trending Toloncha fault and fold system and Peine fault is interposed in the center of the southeastern slope forming a major hydrogeologic feature that likely diverts groundwater as well as generally restricts

groundwater flow through this zone (Breitkreuz, 1995; Jordan et al., 2002; Reutter et al., 2006; Gonzalez et al., 2009; Boutt et al., 2018). The fold and thrust belt architecture of the basin slope is manifested in several thrust fault systems of varying depths and length but which generally trend N-S, parallel to the SdA salar margin; these faults are thought to be major conduits for groundwater flow to the surface as evidenced by the spring complexes emerging along or in the immediate vicinity of these fault zones (Aron et al., 2008; Jordan et al., 2002). Other important fold and thrust features are the Tilocalar Peninsula, which juts out into the middle of the southern transition zone, as well as the monoclinal folded ignimbrites to the south. At the salar scale, faults in the subsurface may act as conduits or barriers to fluid (brine) movement.

2.2 Geology and Hydrogeology of Transition Zone

The transitional zones of salars in the region are known to be composed of a combination of alternating sequences of evaporite deposits (ie. carbonates, sulfates, and chlorides), minor clastic material (clay, silt, sand, and gravel), and in many cases volcanic ash and ignimbrite deposits. In the SdA basin, these geologic units make up the Vilama Formation, the stratigraphy of which is detailed in Lin et al. (2016). The Vilama Formation is up to 1 km thick in places and thickens from the salar margin towards the basin. Figures 1 and 2 depict the generalized distribution of the salt crusts in the marginal transition zones of SdA including the lagoon systems. Salt crust distribution can also be observed in the virtual field trip (Movie S1). Although this paper will focus on the details of a hydrogeochemical transect in the south of the basin (Figure 2) primarily because of the robust data set collected in this region, we will also briefly explore the east transition zone and the associated lagoons (Figure 1).

Lagoon systems may have subtle differences in the specific hydrogeologic setting with respect to how large the diffuse groundwater regions are that transition to focused inflow. The overall morphology and the extent of flooding surfaces of the lagoons may vary, but similar processes described in this paper can apply to other lagoon systems. The SdA marginal transition zone highlights the variability in lagoon morphology as well as the regions between the lagoons and the nucleus margin. For example, the north Chaxa and Barros Negros lagoon systems in the northeast transition zone (Figure 1) appear to be fed by a large diffuse groundwater region that becomes channelized into a small stream that feeds three lagoons which are connected by small

channels. Undoubtedly, this lagoon system also receives inflow from the eastern alluvial fans as small marshes and springs are observed to the east of these lagoons (Ortiz et al. 2014). In some locations, there are distinct spherical dissolution features that can be seen within the lagoons. These likely represent regions where focused groundwater discharge upwells into the marginal transition zone from longer flow paths. Further to the south, the Aguas de Quelana lagoon system (Figure 1) is composed of a series of elongated north-south trending lagoons that occur to the west and down gradient of the massive alluvial fans associated with the very large Tumisa stratovolcano.

Important to understanding the functioning of the transition zone and lagoon systems is the fact that they are underlain by complex heterogeneous subsurface geology that is inherent in the evaporite deposits (Smoot and Lowenstein, 1991; McKnight, 2019) and interbedded ignimbrites, ashes, and clastic material which together form the aquifer system. The supporting document (S1) contains the detailed descriptions of the transition zone subsurface geology that aided in the development of the conceptual model presented in Figure 8.

The hydrostratigraphy of the carbonate, sulfate, and chloride deposits is variable in the lateral and vertical dimensions and is important for understanding why the inflow water discharges in the observed locations and the pattern of the surface distributions. The hydraulic conductivity of these materials is summarized in Figure 8.

There are numerous faults located in the south margin of SdA which have been mapped, measured, and inferred by others (ie. Jordan et al. 2007, Martinez et al. 2018, Rubilar et al. 2018) and have been compiled here (Figures 1 and 2) and extrapolated in the conceptual model (Figure 8) based on high resolution seismic and electrical resistivity surveys and where possible checked against drill cores. Characteristic of the fault zones identified in drill core are zones of fault gouge and breccia that represent damage zones in the area of the faults. We interpret that in at least some areas these faults could act as fluid transport pathways and are responsible to some extent for the movement of recharged water as well as brines (see Figure 8, fault zone conceptualization).

Previous work by Munk et al. (2018) defined that 21% of the water flux in the entire SdA basin discharges to the southern transition zone and lagoon systems and that the entire basin contributes 3.11 m^3/s to all of the lagoon systems in SdA including the south and east lagoons.

The Punta Brava Lagoon Complex (PBLC) is representative of 0.51 m^3/s (GW2 and GW3 from Munk et al., 2018) out of the 4.81 m^3/s of total recharge in the basin and the Salada-Saladita-Interna (SSI) lagoon system fed by the southeast inflow is representative of 0.48 m^3/s (SW/GW1, SW/GW2, GW4 from Munk et al., 2018) making these lagoon systems of particular interest and of focus for this study

3 Materials and Methods

3.1 Sampling and Materials

Water samples used for the PBLC transect analysis (data in Figure 3) were collected for major and minor elements, anions, water stable isotopes, Sr isotopes, and tritium analyses over the period of 2012-2016 by our team. Shallow groundwater samples were obtained from 4" PVC constructed wells with known screened intervals in the upper fresh to brackish regime generally decimeters below the ground surface and with specific conductivity (SC) values of up to 60,000 µS/cm. The deeper brine regime had SC values exceeding 200,000 µS/cm. All surface and groundwater samples were collected into clean HDPE bottles after filtering through a 0.45 µm filter. Samples for major and minor element analysis were acidified with high purity concentrated HNO_3. In-situ measurements of temperature, SC, and pH were made at each sampling location at the time of sample collection with a hand-held YSI multi-probe.

3.2 Geochemical and Isotopic Analyses of Waters

The concentration of major and minor elements in the water samples were analyzed using inductively coupled plasma mass spectrometry (ICP-MS) with a reaction cell for major elements and Li (ICP RC-MS, Agilent 7500c) and anions by ion chromatography (Dionex ICS 5000+) at the University of Alaska Anchorage. Waters with relatively higher TDS were diluted volumetrically prior to analysis. For ICP RC-MS analysis, samples were acidified to 1% HNO_3 v/v prior to analysis. Quantification was performed using seven external calibration standards ranging from 0.1 to 100 ppb. Drift correction was achieved by online addition of 10 ppb of a four element internal standard mix (Li(7), Y, Ce, and Bi). Calibration verification standards and

blanks were run every 10th analysis. Element analysis was verified with external NIST standard SRM 1643d. Samples that exceeded the calibration by 120% were diluted and reanalyzed.

Water samples were analyzed for δ^2H and $\delta^{18}O$ using a Picarro L-1102i WS-CRDS analyzer (Picarro, Sunnyvale, CA) in the ENRI Stable Isotope Laboratory at the University of Alaska Anchorage. International reference standards (IAEA, Vienna, Austria) were used to calibrate the instrument to the VSMOW-VSLAP scale and working standards (USGS45 : δ^2H= -10.3 ‰, $\delta^{18}O$= -2.24 ‰ and USGS46 : δ^2H= -235.8 ‰, $\delta^{18}O$= -29.8 ‰) were used with each analytical run to correct for instrumental drift. Long-term mean and standard deviation records of a purified water laboratory internal QA/QC standard (δ^2H= -149.80 ‰, $\delta^{18}O$= -19.68 ‰) yield an instrumental precision of 0.93 ‰ for δ^2H and 0.08 ‰ for $\delta^{18}O$.

Strontium concentrations and $^{87}Sr/^{86}Sr$ were measured at the University of Utah Strontium Isotope Geochemistry Laboratory following methods described by Chesson et al. (2012). During the course of analysis measurements of the isotopic standard SRM 987 yielded a value of 0.710301 ± 0.000007 (1σ, n=51). Details of methodology are provided in S1 text.

All other geochemical data used in this paper originated from an internal industry report. These data generally represent quarterly sampling over a period of up to a decade and are used primarily in establishing seasonal variability and for modeling saturation indices for each hydrogeochemical zone defined in this work. All data including that collected by the authors and from the industry report can be accessed at (https://doi.org/10.7275/qr40-z439). In-situ measurements of temperature, pH, and SC are reported as well as major and trace element concentrations and anion concentrations. Methods of analysis for the data from the industry report for are for major elements by ICP-OES, minor/trace elements by ICP-MS and anion concentrations by IC, bicarbonate was measured by titration in the laboratory. SGS and ALS commercial geochemical laboratories were utilized for these analyses.

3.3 Geochemical Equilibrium Modeling

The data and detailed methods and results for the equilibrium geochemical modeling are contained in the supporting document for this paper. In summary, two different ionic strength/activity approximations were used for the data set, one for inflow waters with ionic

strength less than 0.1 (Debye-Hückel) and for brackish and brine waters with ionic strength greater than 0.1 (Harvie-Moller-Weare). Equilibrium modeling of saturation indices for the major evaporite minerals observed in the field and drill core (calcite, gypsum, and halite) as well as other mineral phases determined in the modeling predictions are included (Text S1).

3.4 Remote Sensing of Water Bodies

Thirty-meter resolution imagery was downloaded and processed via the LandsatLook Viewer (USGS) for Landsat 7 (1999–present) and Landsat 8 OLI (2013–present). Four images at quarterly increments from years 2003–2016 were analyzed for water coverage extent if possible (January, April, July, October) during the middle of each respective month. If a satellite image during the intended date is unavailable, the next available date is used. All images were imported into ArcGIS and projected to the World Geodetic System 1984 UTM, Zone 19 and overlain on the 30m resolution Land/Water Boundary Time Series (1990–2010) (ESRI). Polygons of the area of lagoons and transitional pools were manually digitized using the Land/Water Time Series base map as a quality control parameter. These features were lumped and associated into their respective groupings. Presence/absence of water is evaluated using qualitative assessment of pixel color. Polygon surface areas are then calculated in square meters. A second interpreter digitized ~3% of the images processed and the calculated differences in areas were within 5% of each other on average. Nucleus margin changes were assessed using LandSat data by digitizing the dark nucleus margin position against the lighter colored modern salt crust. Comparisons are made to legacy geologic maps such as Moraga et al. (1969). Meterological data were obtained from the Peine station from the Chilean Dirección General de Aguas (DGA). Mean daily and monthly precipitation data downloaded from the DGA (http://explorador.cr2.cl/).

4 Results

4.1 Physical and Geochemical Evolution of Inflow, Transition, and Nucleus Waters

Figure 3 illustrates the variation in multiple physical and geochemical parameters of shallow groundwater, the PBLC, transitional pools and the halite nucleus. For reference we use the location of the lagoons as the 0 km point and measure the locations of all the sampling points relative to that up gradient and down gradient (Figure 2). Average concentrations from each sampling point over multi-year periods are used to construct these transects in order to capture

natural variability as there are seasonal and event (precipitation) driven fluctuations. The objective is to indicate the general evolution of the water along the 30 km flow path and the distinctions between water compartments in the marginal transition zone and the edge of the halite nucleus. The deep TZ brines are not included in this transect but are addressed separately.

The shallow groundwater inflows located about 15 km up gradient of the lagoon discharge point are the most southern inflow waters. These are characteristic of the shallow groundwater system with SC values generally less than 5,000 µS/cm, high temperatures, highly negative $\delta D\text{-}H_2O_{VSMOW}$ signatures, ^3H values near zero, low Li and Na concentrations (<10 mg/L and <1000 mg/L respectively) and the least radiogenic but somewhat variable $^{87}Sr/^{86}Sr$ signatures.

Between the shallow groundwater inflow zone (shaded blue) and the lagoons (shaded purple), there is an intermediate region of the transition zone where shallow groundwater is impacted by evaporation, thereby increasing the SC by an order of magnitude, lowering the temperature by more than 10 ^oC, increasing the $\delta D\text{-}H_2O_{VSMOW}$ signature, and increasing both Li and Na concentrations by up to an order of magnitude. From here, the water flows into the lagoons through both diffuse and focused discharge where the water is further exposed to the effects of evaporation in the open water bodies. This is exemplified by an additional order of magnitude increase in SC, although some of this could also be due to interaction with salts that are precipitating and dissolving in this dynamic system (see section 4.2), evaporation is the main driver of these processes on short and long-time scales. The temperature in the lagoons increases due to direct exposure to solar radiation dependent on time of day and since those are surface water body temperatures they are not included in the area of the lagoons in Figure 3. The $\delta D\text{-}H_2O_{VSMOW}$ signatures increase by over 40 ‰ in the open lagoon water, this dramatic increase is explained by the high evaporation rates at the salar surface. Tritium also increases in the lagoons because of the impacts of direct precipitation (Boutt et al., 2016) mixing with the evaporated water. Lithium concentrations increase by about 2-3 times in the lagoons and the Na concentrations increase by another order of magnitude both due to evaporation effects in the open water bodies. Calcium concentrations (not shown) are more variable in the lagoons because of the active precipitation of $CaCO_3$ and $CaSO_4 \cdot 2H_2O$ which can be observed forming in the lagoons typically influenced by the presence of stromatolites.

The water in the region between the lagoons and the transitional pools/nucleus edge as compared to the lagoon water is characterized by an order of magnitude drop in SC, lower $\delta D\text{-}H_2O_{VSMOW}$ signature by 20 ‰, generally lower ^3H, Li concentrations 2-3 times lower and Na concentrations an order of magnitude lower indicating an extreme distinction between this water and the lagoon water.

The transitional pool water that accumulates at the edge of the halite nucleus in a 2-3 m deep trench-like feature formed by dissolution of halite by fresh rain water is another geochemically distinct body of water (Movie S1). This water and its ^3H composition were first highlighted by Boutt et al. (2016) as being dominated by precipitation events due to its large fraction of modern water as calculated from the ^3H content. This water is characterized as brine based on its SC values of 200,000 + µS/cm, the highest $\delta D\text{-}H_2O_{VSMOW}$ measured in any water along the transect due to going towards complete dryness in the trenches, the highest ^3H values along the transect indicating that a large percentage of this water is modern precipitation, high Li concentrations on the order of 1000 mg/L and Na concentrations as high as the nucleus brines. These water features are some of the most dynamic in the salar system because they are compartmentalized by the dissolution trench that has formed along the nucleus edge. This water may seep into the nucleus some distance as shown by the signature of $\delta D\text{-}H_2O_{VSMOW}$ of the transitional pool water and the decrease in this signature to 5 km distance into the halite nucleus. The nucleus brines have been shown to have enriched $\delta D\text{-}H_2O_{VSMOW}$ signatures along the margin but are generally depleted further salarward (Boutt et al., 2016). The dynamic nature of the transitional pools and the lagoons is further documented by analysis of satellite images before and after a major rain event at the salar in 2015 in section 4.3 of this paper.

Finally, the nucleus brines are characterized by the highest SC values, intermediate temperatures and $\delta D\text{-}H_2O_{VSMOW}$ signatures, low to no ^3H, and the highest Li and Na concentrations (with the exception of higher Na concentrations in the transitional pools because of the extreme evaporation that occurs there). In particular, the large difference in the $\delta D\text{-}H_2O_{VSMOW}$ signature of the brines as compared to the lagoon water and the fact that there is no ^3H in the brines defines this water as distinct from the lagoon water.

4.2 Geochemistry of Inflow, Transition Zone and Nucleus Waters

The geochemistry of the waters used in this study aid in defining and classifying the water types of the freshwater-brine system (Figure 4). Using the general flow path physical and chemical trends in Figure 3, the conceptual model (Figure 8), and field observations (Movie S1), we define seven hydrogeochemical zones in the inflow-transition zone-nucleus system. These zones are: 1) inflow (fresh), 2) TZ (transition zone) shallow (fresh to brackish), 3) TZ deep (brackish to brine), 4) lagoon (brackish), 5) TZ margin (brackish to brine), 6) nucleus margin (brine), and 7) nucleus (brine). The brines generally vary between Na-Cl to Na-Ca-SO_4-Cl type. The major elements, anions, Li, and $^{87}Sr/^{86}Sr$ of each zone indicate that the shallow groundwater evolves along the flow path (Figures 3 and 4). Lithium, Na, and K concentrations have similar variability across zones, but are notably on average higher in the nucleus brines compared to the TZ deep brines. Magnesium concentrations have a similar pattern to the alkali metals however, Ca appears to be more variable between the zones, and in particular is lower in the TZ deep brines compared to the nucleus brine with a larger range in the lagoon waters. Chloride concentrations are low in the inflow waters, increase in the lagoons with significant variability, are relatively consistent among the TZ margin, nucleus margin and the nucleus waters and somewhat lower with a large range in the TZ deep brines. Sulfate is also lowest in the inflow waters with an increase in concentration and variability in the lagoons and the marginal waters in the TZ and TZ margin. It is higher in the nucleus brines with less variability as compared to the TZ deep brines. Bicarbonate concentrations are the least variable across zones but like most of the geochemical parameters on average are lower in the TZ deep brines compared to the nucleus brines. Interestingly, the inflow waters, lagoons and TZ deep brines all have similar average bicarbonate concentrations. The $^{87}Sr/^{86}Sr$ signatures of the inflow waters and lagoons on average are similar with the inflow waters having the most variability. The marginal waters are also similar but the nucleus brines and TZ brines indicate a more variable and radiogenic signature and the nucleus brines have a less radiogenic signature than the TZ deep brines. This pattern may be attributable to the diversity in aquifer materials for the brines which include the 3.1 Ma Tucucaro ignimbrite. Subsurface diamond drill cores that intercept the ignimbrite in both the TZ deep brine region and

the nucleus show pervasive alteration of the pumice and glassy matrix in the regions saturated with brine.

In order to further test the processes impacting the water geochemistry along the flow path described in Figure 3 as well as the brines and the marginal waters, equilibrium geochemical modeling was performed on the waters from each of the defined zones (Figure 5). Vasquez et al. (2013) demonstrated the importance of including geochemical reactions for 2D groundwater flow models for a transect in the northeast part of the SdA. They found that because of the formation of secondary minerals in the shallow subsurface, the primary porosity and permeability of the aquifer materials could be altered significantly. The analysis performed in the current work has the objective of using natural water chemistry and testing which minerals are at or near equilibrium to support our observations of secondary mineral precipitation in surficial deposits and those from the diamond drill cores in the subsurface of the southern transition zone.

Figure 5 illustrates the results of the equilibrium geochemical modeling for all of the water zones along the southern margin of the SdA transect for calcite, gypsum and halite. The data used for this modeling were split into those with ionic strength < 0.1 and those with ionic strength > 0.1 (Table S1, Text S1). The lower and intermediate ionic strength waters modeled include those from the inflow and the transition zone and indicate that not only are common evaporite minerals predicted to be stable, but also some silicates as the activity of $SiO_{2(aq)}$ is high enough in these regions to form silicate phases. There are some 1-5 cm lenses of dense chert-like material that appear to be post depositional which are found within the cores in the transition zone. A sample of this material has been identified as containing trydimite by XRD methods (J. Grotzinger, pers. comm.). The results from the inflow water modeling are similar to those for inflow waters found further upgradient by 10s of km in the same aquifer (MNT) as reported in Rissmann et al. (2015) (discussed in Text S1). For waters in the lagoons, TZ margin, nucleus margin, and halite nucleus, we report the range of saturation indices for calcite, gypsum and halite as those are the dominant mineral phases observed in the field from surface mapping and in the subsurface from drill core (Text S1).

Along the flow path, the general trend indicates that the inflow and transition zone waters are undersaturated with respect to halite and gypsum (log Q/K < 0) but are at saturation with respect to calcite (log Q/K > 0) and other carbonate, sulfate and silicate minerals (Table S1). The lagoon waters which are represented here by waters from Laguna Brava are undersaturated with respect to halite but are at saturation with respect to calcite and to a lesser extent gypsum. The TZ margin, nucleus margin, and the nucleus waters are all saturated with respect to halite, gypsum, and calcite, indicating that it is in these regions that concentrations/activities of the required ions are elevated enough to cause the precipitation of all mineral phases at least over the seasonal timeframes. It is also apparent that the lagoon, transition zone, and nucleus edge waters have the most range in SI values which is expected because these waters are more susceptible to mixing from precipitation events and effects of evaporation given that they are exposed at the surface or contain components of water that are exposed at the surface. It is worth noting here that in the field there are areas within the transition zone that display vadose zone processes are at work including formation of secondary mineral precipitates such as efflorescent salts and chlorides that are precipitating within cracks and other openings in the primary salt crusts, attributable to evaporation processes and the continual delivery of solutes above the water table to form secondary minerals.

4.3 Temporal Dynamics of Transitional Pool and Lagoon Waters

The edge of the halite nucleus along the southern margin of SdA is characterized by a ~ 2 m wide depression that fills with water from precipitation events on or near the salar surface, these features are defined as the transitional pools (Boutt et al., 2016). The transitional pools form from the dissolution of the halite primarily by fresher rain water and likely from smaller amounts of shallow locally-derived groundwater emerging from alluvial fans on the west and east side of the Cordon de Lila (^{3}H observations from Boutt et al., 2016 and Figure 3 from this work). Over time the water in the depression evaporates resulting in stable water isotopic signatures that are highly enriched (Boutt et al., 2016) compared to the nucleus brine. These pools frequently evaporate to complete dryness during the austral summer which is accompanied by precipitation of secondary minerals including halite. Figure 6 illustrates the southern margin of SdA over the time period from 1969-2014. It is compiled from the oldest published geologic map (Moraga et

al., 1969) that depicts the transitional pools combined with the January 2014 Landsat image. The outline of the position of the edge of the nucleus margin/transitional pools is based on the 1969 map, the 1999 position and the 2014 position from Landsat imagery. The results of this analysis indicate two important observations: 1) the transitional pool features have persisted through time at least back to 1969 prior to the onset of any brine extraction from the halite nucleus, and 2) the most apparent change to the position of the nucleus edge occurred between 1969 and 1999 and less change is detectable between 1999 and 2014.

Satellite imagery and geochemical and isotopic analyses of lagoon waters indicate that the lagoons are seasonally dynamic features that are supported by shallow groundwater discharge but also respond to local precipitation events (Boutt et al., 2016). Figure 7a depicts the surface area extent of surface water bodies in the southern transition zone before and after a major precipitation event that occurred on the salar in March 26, 2015. The result was a growth in surface area of all the surface water features by a factor of 2.7. Lagoon surface area extent changed from 0.9 km^2 to 1.6 km^2, an increase of 77% which is about 25% higher than the change over an annual cycle caused by incident solar radiation. The transitional pools grew by over 250% after the precipitation event changing in size from 0.33 km^2 to 1.28 km^2.

The longer term (2002-2016) annual variation in surface area of both the PBLC and SSI lagoons and the transitional pools along the nucleus margin as well as daily precipitation recorded at the DGA Peine meteorological station (located on the southeast of the Salar) are illustrated in Figure 7b. These changes were first highlighted by Boutt et al. (2016) but are also demonstrative in this analysis because these observations indicate the annual and decadal dynamic behavior of the surface water bodies in the transition zone. Overall the SSI lagoon system appears to have the least amount of natural variability as compared to the PBLC system and the transitional pools along the nucleus margin. This type of analysis combined with other ground-based observations is fundamental in the overall understanding of water use and its impacts in this basin. For example, in order to assess the impact of groundwater pumping of brine or freshwater on the surface water bodies, the natural responses of these water bodies to hydrologic events provides the baseline from which to assess other impacts.

5 Discussion

5.1 Flow Path Evolution

In order to have appropriate geologic and hydrogeologic context for interpretation of the geochemical properties of each water type in the freshwater-brine system of a salar, a detailed understanding of the subsurface is required. Figure 8 is a 3D hydrogeologic conceptual model of a section through the inflow zone to the halite nucleus. This model is an integrated conceptualization of all of the water zones, flow paths, subsurface geology (including major faults), and hydrogeologic property variability and heterogeneity. It represents the synthesis of detailed (1 m scale) core logging to identify lithologies, observations of secondary mineral occurrence and primary and secondary porosity, correlations of mapped surface and subsurface geology, and hydrogeologic observations and measurements. The result is a comprehensive framework to interpret both hydrogeologic and geochemical observations and processes.

The water discharging in the vicinity of the lagoons flows along long flow paths discharging from the inflow region into the TZ shallow zone (Figure 8). As water enters this region it begins to undergo physical and chemical transformations due to the proximity of the water with the land surface. Evaporation, mineral precipitation, and dissolution cause the water to increase in TDS. Flow paths into the region have both a horizontal and vertical component as depicted with arrows in Figure 8. The presence of evaporite deposits with varying permeabilities causes the flow paths to converge on the TZ shallow region until they reach 1-2 m below ground surface. At this depth, evaporation begins to remove water from the system driving mineral precipitation in the general order of carbonate in the marshes and further salarward additional equilibrium with gypsum and halite is reached, although as demonstrated by the equilibrium geochemical modeling of samples collected seasonally, carbonate equilibrium may be reached across all water types.

There are a number of discrete flow paths into the TZ shallow zone that discharge at varying rates and locations throughout this area. Some of the water forms springs that discharge at rates greater than the rate at which evaporation can remove the water into the atmosphere. Water does not pool everywhere on the surface in this zone for two reasons: 1) discharge appears to be

smaller than the soil evaporation and 2) once water is present at the surface evaporation rates increase substantially resulting in a non-linear feedback. Because evaporation varies seasonally, some seeps with lower inflow rates are ephemeral and form small lagoons that are seasonally present. The predominant discharge locations occur in the regions up hydraulic gradient of the lagoons. Here the discharge rates are high enough that the rate of discharge greatly exceeds evaporation forming large perennial surface water features which are the lagoons. Even though there are local seeps in and around the margin of lagoons, the majority of water flux into the lagoons appears to be upgradient of the actual surface water feature. Boutt et al. (2016) and Moran et al. (2019) showed that water discharging to these lagoons is a complex mixture of regional groundwater and modern precipitation. The results presented here indicate considerable seasonal variability in the geochemistry of the lagoon waters. Tritium analyses of lagoon waters show that the lagoons at any one time can have up to 30% modern water highlighting the importance of sporadic precipitation events on the hydrologic budget of the lagoons, even though over the long term most of the water is sourced from older regional flow paths (Boutt et al., 2016).

5.2 Geochemical Evolution of Waters in Transition Zone

The physical and chemical transect of the shallow freshwater-brine system in Figure 3 indicates that the shallow groundwater system evolves from fresh to brackish to brine waters over a long flow path originating in the upgradient MNT aquifer which is the primary source of inflow water. Generally, the groundwaters in and around the lagoons show significant spatial variability but have much less seasonality than the lagoon waters themselves because they are sustained from inflow waters derived from the MNT aquifer to the south and are not as responsive to evaporation as the open water bodies. Previously, Munk et al. (2018, Fig. 8) demonstrated that the lithium brine in the nucleus is formed over timeframes of millions of years from water-rock interaction in the inflow zones followed by concentrating processes of evaporation and ultimately by halite fractional crystallization causing the residual brines to become highly enriched in Li which is also extremely incompatible. The work presented in this contribution further exemplifies that the TZ regions of salars are unique and independent hydrogeologic functioning areas that are separate from the thick less hydrogeologically active nucleus. This is

demonstrated by the lack of hydrogeochemical connection between the lagoons, the TZ margin, and the nucleus margin waters (Figure 3). Recharge to the halite nucleus does happen (Boutt et al., 2016) but is primarily through waters that accumulate along the halite nucleus margin in transitional pools as well as through direct precipitation on the salar surface.

Waters in the zone between the lagoons and halite nucleus edge are easiest explained as being a mixture of modern precipitation and shallow regional groundwater. In fact, if the lagoons did not exist and their waters were removed from the transect in Figure 3 the intermediate waters between the lagoons and the transitional pools/halite nucleus edge would appear to be a mixture of inflow water and brine. However, the lagoons do persist because of constant shallow groundwater discharge and low permeability geologic units in the subsurface (Figure 8) combined with effects of high evaporation rates.

The major element and anion plus Li concentration data for all of the defined water zones in the system further illustrate the lack of similarity between the inflow and TZ shallow waters as compared to the lagoons, TZ margin, nucleus margin, and the brines (Figure 5). The compartments that appear to have distinct geochemical cohesion are 1) the inflow and shallow TZ, 2) lagoons, 3) TZ margin, TZ deep and nucleus margin, and 4) nucleus. Munk et al. (2018) indicated that the difference between the inflow/TZ shallow waters and the lagoons could easily be explained by evaporation of the inflows to reach concentrations observed in the lagoons, which holds in this expanded dataset as well. However, the current analysis also indicates that the waters salarward of the lagoons and upgradient of the nucleus are also distinct in this system but similar to each other whereas the nucleus brines have their own geochemical signature and are distinct from the TZ brines.

The $^{87}Sr/^{86}Sr$ signatures indicate that there is subsurface weathering/dissolution water-rock interaction with a radiogenic source, likely the Tucucaro ignimbrite or other volcanic deposits. However, the $^{87}Sr/^{86}Sr$ show some variability in the inflow region indicating that there could be some mixing of water sources within the south inflow region, and/or this could be representative of the shallow groundwater transitioning from the alluvial fan material aquifer into the ignimbrite aquifer. Isotopic and geochemical data presented by Garcia et al. (2020), Godfrey et

al. (2019) and Godfrey and Alvarez-Amado (2020) also subsequently support this interpretation. Not only is this subsurface process likely a major mechanism for Li and other elements to be released to the brine, but it also contributes to increasing the porosity and permeability of the ignimbrite as a potential aquifer. The waters in the transition zone, the lagoons and nucleus maintain higher $^{87}Sr/^{86}Sr$ signature. Munk et al. (2018) determined that the sources of water from the south part of the SdA basin and the brines found at elevation all have a very similar $^{87}Sr/^{86}Sr$ signature as the brines in the south part of the halite nucleus.

There are two critical findings from this data and analysis: 1) the inflow and TZ shallow waters are distinct from a subsurface brine that occurs in the TZ deep region, and 2) the TZ deep brines are geochemically distinct from the nucleus brines indicating that overall the TZ appears to be hydrogeologically distinct from the nucleus in both the shallow groundwater system and the deeper brine groundwater system. McKnight (2019) build on these observations to further model the decoupling of the freshwater-brine interface and demonstrate that it is critical to use heterogenous modeling approaches to best represent these systems. The new detailed subsurface geology that has been interpreted (Figure 8) also supports these findings given the large range of hydraulic conductivities of this aquifer system.

The results of the geochemical equilibrium modeling presented in Figure 5 indicate that there are definitive zones of predictable mineral precipitation in the freshwater-brine system but that there is considerable variability particularly in surface water bodies directly exposed to the influence of evaporation. Halite saturation is apparent only in the nucleus, nucleus margin, TZ margin and some of the TZ deep brines. Gypsum saturation occurs within those same waters but also in some lagoon waters and calcite saturation occurs across all water zones. Even though we observe certain geochemical zones in the field that are dominated by carbonate, gypsum and halite, the equilibrium geochemical modeling of a dataset spanning a decade with samples collected seasonally suggests that there is variability in the saturation states of waters across the zones. The TZ deep brines are also distinct from other brines in the system showing a much larger variability in geochemical composition and predicted saturation states. The later finding is critical as TZ brines are generally understudied, but because they appear to be distinct from the nucleus brines there maybe additional/different processes responsible for their formation. The

equilibrium modeling also aids in verifying the role of secondary mineral precipitation on the hydrogeologic properties of porosity and permeability in the aquifer system of the TZ as depicted in Figure 8 and suggested by reactive transport modeling of Vasquez et al. (2013).

5.3 Spatial and Temporal Dynamics of Groundwater Discharge Features and Transitional Pools

The hydrodynamic behavior of the lagoon systems in the transition zone is dependent on support from groundwater discharge derived upgradient, annual fluctuations in evaporation and direct precipitation on the salar. The transitional pools along the halite nucleus margin have a distinct hydrodynamic behavior from that of the other open bodies of water in the transition zone. This is because the later are not supported by continued groundwater discharge but rather primarily respond to precipitation events on the salar surface. This is a major distinction between the lagoons and the transitional pools indicating their general lack of hydraulic connection. The remote sensing analysis of the open bodies of water in the transitional areas of the salar further reveal the importance of precipitation events and climate on the size of these water bodies.

5.4 Application to Other Salars

We present a new look at salar freshwater-brine systems with a focus on the transitional zone where freshwater inflow terminates. From the work presented at Salar de Atacama we propose that for Andean salars in the Altiplano-Puna region there are three main points about how the salar and marginal salar systems function: 1) subsurface geology of transition zones has varying complexity and is responsible for the formation of surface water bodies, 2) lagoons that may exist on the margin of salars can persist for millions of years and have their water sourced from a combination of long (old) flow paths as well as pulsed recharge from modern precipitation events, and 3) lagoons and other freshwater sourced features that are persistent, such as springs and marshes may be distinct geochemically but can also be highly compartmentalized and disconnected from the halite nucleus (core of the salt pan) and associated brines, but do rely on the influx of freshwater from upgradient sources. Although salars in other regions of the world may have differences in these characteristics resulting from variability in climate, geology,

hydrology and other aspects, this basic framework can be used as a reference for approaching the functioning of salars on a global scale.

6 Conclusions

This work provides new insights into quantifying the relationship between the hydrogeological and geochemical zones of salar freshwater-brine systems, as exemplified by the SdA system. A pivotal finding from this research is that complex subsurface geology and the development of a freshwater-brine interface control the formation of the defined water zones, including marginal lagoon systems that are vital ecosystems. These important observations made through a complete assessment of all water types through the salar freshwater-brine system are supported by physical, geologic, geochemical, and isotopic evidence. Assessing the sustainability of the nucleus brine and freshwater resources in this region is dependent on this type of integrated approach and scientific analysis. These new observations and findings are particularly important in understanding the position and dynamic behavior of lagoons and other surface water bodies in the transitional zone of salar systems. The lagoons grow and shrink in response to climate and precipitation, are perched by low permeability materials in the subsurface and are dependent on freshwater inflow from the southern aquifers (MNT), not on the position of the freshwater-brine interface in the subsurface. Geochemical differences in the transition zone brine and the nucleus brine indicate that there may be other processes responsible for the formation of the TZ brine as compared to the nucleus brine.

7 Acknowledgments and Data

The authors would like to thank Albemarle for providing access to diamond drill cores for analysis as well as access to their internal database of water chemistry and for general support of the research, particularly for field operations. Contributions to the remote sensing analysis from Lilly Corenthal, Leah Santangelo, and Anna Campbell are gratefully acknowledged. Three anonymous reviews helped improve the quality of this manuscript. This project was also partially supported by NSF award 1443226. There are no real or perceived financial conflicts or interests

for any of the authors. Data supporting the conclusions can be obtained from https://doi.org/10.7275/qr40-z439.

Figure Captions

Figure 1. Landsat image of the Salar de Atacama with major surface salt crust zones shaded and outlined (carbonate, gypsum, and halite) and major lagoon systems identified (dark blue). Lagoons include the Punta Brava Lagoon Complex (PBLC), the Salada-Saladita-Interna (SSI) lagoon system, the Aguas de Quelana lagoon system, and the Chaxa and Barros Negros lagoon systems. The major faults and folds of the region are also identified (dashed where interpreted). Sampling locations with data reported in this study are shown as black dots.

Figure 2. Detailed Landsat image of the southern SdA with major surface salt crust zones shaded and outlined as in Figure 1. Major lagoon systems, wetlands, and the transitional pools are identified. The detailed hydrogeochemical transect depicted in Figure 3 and 8 is shown as a white line that runs from the upgradient inflow zone through and across the transition zone and nucleus margins to terminate in the halite nucleus. Please note that regions of inflow, transition zone (TZ) shallow and deep, lagoons, TZ margin, nucleus edge, and nucleus are also highlighted in Movie S1 for a virtual field trip across these zones.

Figure 3. The 30 km hydrogeochemical transect spanning the freshwater-brine salar system (transect location depicted in Figures 1 and 2). The PBLC location is used as the 0 km measuring point for up gradient and downgradient distances. Blue shading denotes the inflow water zone, purple the lagoons, and light blue is the transitional pools and edge of transition zone margin and halite nucleus. Temperature data for surface water bodies are not included due to diurnal variability. Specific conductivity and ^{3}H (Rmod) first published in Boutt et al. (2016).

Figure 4. Chemical composition of major elements, anions, Li and $^{87}Sr/^{86}Sr$ signatures in all water compartments including all sampling events for this study. Inset representative cross section simplified from the conceptual model in Figure 8.

Figure 5. Histograms of predicted Log (Q/K) saturation indices for major evaporite phases for all of the water compartments in the freshwater-brine system including subsurface brines found under the transition zone (TZ deep) for multi-year/seasonal data. All modeled SI data are included in Table S1.

Figure 6. Section of the geologic map from Moraga et al. (1969) for the southeast part of SdA overlain on the January 2014 Landsat image with the position of the nucleus edge/transitional pools in the years 2014 (yellow), 1999 (orange), and 1969 (red). Mapped geologic unit abbreviations can be found in Moraga et al. (1969).

Figure 7a-b. Top panel (a) Landsat image from April 2, 2015 depicting the change in the surface area of surface water bodies in the TZ, TZ margin, lagoons, and nucleus edge before and after a major storm event in March 2015. Lower panel (b) is long-term change in surface area of the transitional pools and two lagoon systems (PBLC and SSI) in the southeastern SdA area as determined from remote sensing mapping based on Landsat imagery.

Figure 8. Three-dimensional conceptual diagram of the SdA inflow, transition zone, and nucleus water system with the inflow waters to the south and the halite nucleus to the north (see transect

location in Figure 2). Subsurface geology, hydrogeologic flow paths, and groundwater discharge features including the wetlands, springs, lagoons and transitional pools are depicted. Overlain is transparent blue to represent fresher waters while red/pink represents brackish and brine waters. The region under the transitional pools is shaded darker to highlight the area where the secondary porosity and permeability of the halite is thought to be important. Finer scale characteristics such the heterogeneity in the transition zone geology, primary, and secondary porosity and permeability features in the transition zone carbonate, interbedded gypsum and halite, and halite nucleus are detailed in the circular insets. Flow path arrows depict diffuse groundwater movement in the shallow parts of the transition zone that ultimately end in the lagoons. Wider blue arrows indicate the relative amounts of infiltration (downward) and evaporation (upward). Our virtual field trip across the surface of these water zones is in Movie S1.

References

Allmendinger, R. W., Jordan, T. E., Kay, S. M., & Isacks, B. L. (1997). The Evolution of The Altiplano-Puna Plateau of the Central Andes. Annual Review of Earth and Planetary Sciences, 25(1), 139–174. https://doi.org/10.1146/annurev.earth.25.1.139

Alpers, C. N., & Whittemore, D. O. (1990). Hydrogeochemistry and stable isotopes of ground and surface waters from two adjacent closed basins, Atacama Desert, northern Chile. Applied Geochemistry, 5(5–6), 719–734. https://doi.org/10.1016/0883-2927(90)90067-F

Aron, F., González, G., Veloso, E., & Cembrano, J. (2008). Architecture and style of compressive Neogene deformation in the eastern-southeastern border of the Salar de Atacama Basin (22 30'-24 15'S): A structural setting for the active volcanic arc of the Central Andes. In 7th International Symposium on Andean Geodynamics (ISAG 2008, Nice) (pp. 52-55)

Benison, K.C., Goldstein, R.H., (2001). Evaporites and siliciclastics of the Permian Nippewalla Group, Kansas and Oklahoma: a case for nonmarine deposition. Sedimentology 48, 165–188.

Boschetti, T., Cortecci, G., Barbieri, M., & Mussi, M. (2007). New and past geochemical data on fresh to brine waters of the Salar de Atacama and Andean Altiplano, northern Chile. Geofluids, 7(1), 33–50. https://doi.org/10.1111/j.1468-8123.2006.00159.x

Boutt, D.F., Hynek, S.A., Munk, L.A., Corenthal, L.G. (2016). Rapid recharge of fresh water to the halite-hosted brine aquifer of Salar de Atacama, Chile. Hydrol. Process. 30 (25), 4720–4740. http://dx.doi.org/10.1002/hyp.10994.

Boutt, D., Corenthal, L., Munk, L. A., & Hynek, S. (2018). Imbalance in the modern hydrologic budget of topographic catchments along the western slope of the Andes (21–25 S). https://doi.org/10.31223/osf.io/p5tsq

Breitkreuz, C. (1995). The late Permian Peine and Cas Formations at the eastern margin of the Salar de Atacama, Northern Chile: stratigraphy, volcanic facies, and tectonics. Revista Geológica de Chile, 22(1), 3–23.

Carmona, V., Pueyo, J. J., Taberner, C., Chong, G., & Thirlwall, M. (2000). Solute inputs in the Salar de Atacama (N. Chile). In Journal of Geochemical Exploration (Vol. 69–70, pp. 449–452). https://doi.org/10.1016/S0375-6742(00)00128-X

Chesson, L.A., Tipple, B.J., Mackey, G.N., Hynek, S.A., Fernandez, D.P., Ehleringer, J.R. (2012). Strontium isotopes in tap water from the coterminous USA. Ecosphere (3), 67. http://dx.doi.org/10.1890/ES12-00122.1.

Corenthal, L.G., Boutt, D.F., Hynek, S.A., Munk, L.A. (2016). Regional groundwater flow and accumulation of a massive evaporite deposit at the margin of the Chilean Altiplano. Geophys. Res. Lett. 43 (15), 8017–8025. http://dx.doi.org/10.1002/ 2016GL070076.

de Silva, S. L. (1989). Geochronology and stratigraphy of the ignimbrites from the 21°30′S to 23°30′S portion of the Central Andes of northern Chile. Journal of Volcanology and Geothermal Research, *37*(2), 93–131. https://doi.org/10.1016/0377-0273(89)90065-6

de Silva, S. L. (1989a). Altiplano-Puna volcanic complex of the central Andes. Geology, 17(12), 1102–1106. https://doi.org/10.1130/0091-7613(1989)017<1102:APVCOT>2.3.CO;2

Eugster, H.P. and Hardie, L.A., (1978). Saline lakes. In: Lerman, A. (Ed.), Lakes: Chemistry, Geology Physics. Springer-Verlag, pp. 237 – 293.

Garcia, M. G., Borda, L. G., Godfrey, L. V., López Steinmetz, R. L., & Losada-Calderon, A. (2020). Characterization of lithium cycling in the Salar De Olaroz, Central Andes, using a geochemical and isotopic approach. Chemical Geology, 531. https://doi.org/10.1016/j.chemgeo.2019.119340

Gardeweg, M., & Ramírez, C. F. (1987). La Pacana caldera and the Atana Ignimbrite - a major ash-flow and resurgent caldera complex in the Andes of northern Chile. Bulletin of Volcanology, 49(3), 547–566. https://doi.org/10.1007/BF01080449

Gleeson, T., Cuthbert, M., Ferguson, G., & Perrone, D. (2020). Global Groundwater Sustainability, Resources, and Systems in the Anthropocene. Annual Review of Earth and Planetary Sciences, 48(1), 431–463. https://doi.org/10.1146/annurev-earth-071719-055251

Godfrey, L. V., Herrera, C., Gamboa, C., & Mathur, R. (2019). Chemical and isotopic evolution of groundwater through the active Andean arc of Northern Chile. Chemical Geology, 518, 32–44. https://doi.org/10.1016/j.chemgeo.2019.04.011

Godfrey, L., and Álvarez-Amado, F. (2020). Volcanic and saline lithium inputs to the salar de atacama. Minerals, 10(2). https://doi.org/10.3390/min10020201

González, G., Cembrano, J., Aron, F., Veloso, E. E., & Shyu, J. B. H. (2009). Coeval compressional deformation and volcanism in the central Andes, case studies from northern Chile (23°S-24°S). Tectonics, 28(6). https://doi.org/10.1029/2009TC002538

Hardie LA, and Eugster HP., (1970). Evolution of Closed-Basin Brines. Mineralogical Society of America - Special Papers. 273–290.

Hardie LA, Smoot JP, and Eugster HP., (1978). Saline lakes and their deposits: A sedimentological approach. In: Matter A and Tucker ME (eds.) Modern and Ancient Lake Sediments, Special Publication, vol. 2, pp. 7–41. Oxford: International Association of Sedimentologists.

Herrera, C., Custodio, E., Chong, G., Lambán, L. J., Riquelme, R., Wilke, H., … Lictevout, E. (2016). Groundwater flow in a closed basin with a saline shallow lake in a volcanic area: Laguna Tuyajto, northern Chilean Altiplano of the Andes. Science of the Total Environment, 541, 303–318. https://doi.org/10.1016/j.scitotenv.2015.09.060

Houston, J. (2009). A recharge model for high altitude, arid, Andean aquifers. Hydrological Processes, 23(16), 2383–2393. https://doi.org/10.1002/hyp.7350

Houston, J., Butcher, A., Ehren, P., Evans, K., & Godfrey, L. (2011). The evaluation of brine prospects and the requirement for modifications to filing standards. Economic Geology. https://doi.org/10.2113/econgeo.106.7.1225

Houston, J. and Hart, D. (2004). Theoretical head decay in closed basin aquifers: an insight into fossil groundwater and recharge events in the Andes of northern Chile. Quarterly Journal of Engineering Geology and Hydrogeology 37, 131–139. doi:10.1144/1470-9236/04-007

Jordan, T. E., L. V. Godfrey, N. Munoz, R. N. Alonso, T. K. Lowenstein, G. D. Hoke, N. Peranginangin, B. L. Isacks, and L. Cathles (2002), Orogenic-scale ground water circulation in the Central Andes: evidence and consequences., 5th ISAG (International Symp. Andean Geodyn., 331–334.

Jordan, T. E., Mpodozis, C., Muñoz, N., Blanco, N., Pananont, P., & Gardeweg, M. (2007). Cenozoic subsurface stratigraphy and structure of the Salar de Atacama Basin, northern Chile. Journal of South American Earth Sciences, 23(2–3), 122–146. https://doi.org/10.1016/j.jsames.2006.09.024

Jordan, T. E., Nester, P. L., Blanco, N., Hoke, G. D., Dávila, F., & Tomlinson, A. J. (2010). Uplift of the Altiplano-Puna plateau: A view from the west. Tectonics, 29(5). https://doi.org/10.1029/2010TC002661

Lin, Y. S., Chuang, Y. R., Shyu, J. B. H., González, G., Shen, C. C., Lo, C. H., & Liou, Y. H. (2016). Structural characteristics of an active fold-and-thrust system in the southeastern Atacama Basin, northern Chile. Tectonophysics, 685, 44–59. https://doi.org/10.1016/j.tecto.2016.07.015

Martínez, F., López, C., Bascuñan, S., & Arriagada, C. (2018). Tectonic interaction between Mesozoic to Cenozoic extensional and contractional structures in the Preandean Depression (23°–25°S): Geologic implications for the Central Andes. Tectonophysics, 744, 333–349. https://doi.org/10.1016/j.tecto.2018.07.016

McKnight, S. (2019). The Climatic and Hydrostratigraphic Controls on Brine-to-Freshwater Interface Dynamics in Hyperarid Climates: A 2-D Parametric Groundwater Modeling Study, Masters Thesis, 785. https://scholarworks.umass.edu/masters_theses_2/785. https://doi.org/10.31223/osf.io/ea783

Mather, A. E., and Hartley, A. (2005). Flow events on a hyper-arid alluvial fan: Quebrada Tambores, Salar de Atacama, northern Chile. Geological Society Special Publication, 251, 9–24. https://doi.org/10.1144/GSL.SP.2005.251.01.02

Moran, B. J., Boutt, D. F., & Munk, L. A. (2019). Stable and Radioisotope Systematics Reveal Fossil Water as Fundamental Characteristic of Arid Orogenic-Scale Groundwater Systems. Water Resources Research, 55(12), 11295–11315. https://doi.org/10.1029/2019WR026386

Moraga B., Aldo, Chong D., Guillermo, Fortt, María Angélica, Henríquez A., Hugo. (1969). Estudio geológico del Salar de Atacama, provincia de Antofagasta [informe inédito]. Antofagasta: IIG, 155p.

Moraga A., Chong G., Fortt M.A., Henríquez H., (1974). Estudio geológico del Salar de Atacama, provincia de Antofagasta Inst. Invest. Geol. (Chile), Bol., No., 29, p. 59

Munk, L.A., Hynek, S., Bradley, D., Boutt, D., Labay, K., & Jochens, H. (2016). Lithium Brines A Global Perspective.

Munk, L. A., Boutt, D. F., Hynek, S. A., & Moran, B. J. (2018). Hydrogeochemical fluxes and processes contributing to the formation of lithium-enriched brines in a hyper-arid continental basin. Chemical Geology, 493, 37–57. https://doi.org/10.1016/j.chemgeo.2018.05.013

Nesbitt HW, (1974). The Study of Some Mineral-Aqueous Solution Interactions. Unpublished PhD Dissertation, Johns Hopkins University, 173 pp

Ortiz, C., Aravena, R., Briones, E., Suárez, F., Tore, C., & Muñoz, J. F. (2014). Sources of surface water for the Soncor ecosystem, Salar de Atacama basin, northern Chile. Hydrological Sciences Journal, 59(2), 336–350. https://doi.org/10.1080/02626667.2013.829231

Pigati, J. S., Rech, J. A., Quade, J., & Bright, J. (2014). Desert wetlands in the geologic record. Earth-Science Reviews. https://doi.org/10.1016/j.earscirev.2014.02.001

Rettig, S. L., Jones, B. F., & Risacher, F. (1980). Geochemical evolution of brines in the Salar of Uyuni, Bolivia. Chemical Geology, 30(1–2), 57–79. https://doi.org/10.1016/0009-2541(80)90116-3

Reutter, K. J., Charrier, R., Götze, H. J., Schurr, B., Wigger, P., Scheuber, E., ... & Chong, G. (2006). The Salar de Atacama Basin: a subsiding block within the western edge of the Altiplano-Puna Plateau. In the Andes (pp. 303-325). Springer Berlin Heidelberg.

Risacher, F., & Fritz, B. (2009). Origin of salts and brine evolution of Bolivian and Chilean salars. Aquatic Geochemistry, 15(1–2), 123–157. https://doi.org/10.1007/s10498-008-9056-x

Rissmann, C., Leybourne, M., Benn, C., & Christenson, B. (2015). The origin of solutes within the groundwaters of a high Andean aquifer. Chemical Geology, 396, 164–181. https://doi.org/10.1016/j.chemgeo.2014.11.029

Rosen, M. R. (1994). The importance of groundwater in playas: A review of playa classifications and the sedimentology and hydrology of playas. Special Paper of the Geological Society of America, 289, 1–18. https://doi.org/10.1130/SPE289-p1

Rubilar, J., Martínez, F., Arriagada, C., Becerra, J., & Bascuñán, S. (2018). Structure of the Cordillera de la Sal: A key tectonic element for the Oligocene-Neogene evolution of the Salar de Atacama basin, Central Andes, northern Chile. Journal of South American Earth Sciences, 87, 200–210. https://doi.org/10.1016/j.jsames.2017.11.013

Salas, J., J. Guimerà, O. Cornellà, R. Aravena, E. Guzmán, C. Tore, W. Von Igel, and R. Moreno (2010), Hidrogeología del sistema lagunar del margen este del Salar de Atacama (Chile), Bol. Geol. y Min., 121(4), 357–372.

Sancho-Tomás, M., Somogyi, A., Medjoubi, K., Bergamaschi, A., Visscher, P. T., Van Driessche, A. E. S., … Philippot, P. (2018). Distribution, redox state and (bio)geochemical implications of arsenic in present day microbialites of Laguna Brava, Salar de Atacama. Chemical Geology, 490, 13–21. https://doi.org/10.1016/j.chemgeo.2018.04.029

Schmitt, A. K. (2001), Gas-saturated crystallization and degassing in large-volume, crystal-rich dacitic magmas from the Altiplano-Puna, northern Chile, J. Geophys. Res., 106 (B12), 30561– 30578, doi:10.1029/2000JB000089.

Smoot, J.P., and Lowenstein, T.K., (1991). Depositional environments of non-marine evaporites, in Melvin, J.L., ed., Evaporites, Petroleum and Mineral Resources: Amsterdam, Elsevier, Developments in Sedimentology 50, p. 189–347

Spiro, B., and Chong, G., (1996). Origin of sulfate in the Salar de Atacama and the Cordillera de la Sal, initial results of an isotopic study: International Symposium on Andean Geodynamics, 3rd, Paris, Saint Malo, France, Orstom Editions, Collection Colloques et Seminaires, p. 703–705.

Strecker, M. R., Alonso, R. N., Bookhagen, B., Carrapa, B., Hilley, G. E., Sobel, E. R., & Trauth, M. H. (2007). Tectonics and Climate of the Southern Central Andes. Annual Review of Earth and Planetary Sciences, 35(1), 747–787. https://doi.org/10.1146/annurev.earth.35.031306.140158

Tyler, S. W., Muñoz, J. F., & Wood, W. W. (2006). The response of playa and sabkha hydraulics and mineralogy to climate forcing. Ground Water. https://doi.org/10.1111/j.1745-6584.2005.00096.x

Vásquez, C., Ortiz, C., Suárez, F., & Muñoz, J. F. (2013). Modeling flow and reactive transport to explain mineral zoning in the Atacama salt flat aquifer, Chile. Journal of Hydrology, 490, 114–125. https://doi.org/10.1016/j.jhydrol.2013.03.028

Wang, J., Song, C., Reager, J. T., Yao, F., Famiglietti, J. S., Sheng, Y., … Wada, Y. (2018). Recent global decline in endorheic basin water storages. Nature Geoscience, 11(12), 926–932. https://doi.org/10.1038/s41561-018-0265-7

Ward, K. M., Zandt, G., Beck, S. L., Christensen, D. H., & McFarlin, H. (2014). Seismic imaging of the magmatic underpinnings beneath the Altiplano-Puna volcanic complex from the joint inversion of surface wave dispersion and receiver functions. Earth and Planetary Science Letters, 404, 43–53. https://doi.org/10.1016/j.epsl.2014.07.022

Warren, J.K., (2006). Evaporites: Sediments, Resources and Hydrocarbons. Springer, Berlin. 1036 p.

Warren, J. K. (2010). Evaporites through time: Tectonic, climatic and eustatic controls in marine and nonmarine deposits. Earth-Science Reviews. https://doi.org/10.1016/j.earscirev.2009.11.004

Warren, J.K. (2016). Evaporites. In: A Geological Compendium, 2nd ed. Springer Berlin Heidelberg, pp. 1–1035. http://dx.doi.org/10.1007/978-3-319-13512-0.

Wilson, J. L., and Guan, H. (2004). Mountain-Block Hydrology and Mountain-Front Recharge. In Groundwater Recharge in a Desert Environment: The Southwestern United States (Vol. 9, pp. 113–137). American Geophysical Union. https://doi.org/10.1029/009WSA08

WMC [Water Management Consultants Ltda.] (2007). Analisis de la relacion entre las aguas subterraneas del Proyecto Pampa Colorada, las vertientes y del margen este del Salar de Atacama y las Lagunas Miscanti y Minique, Informe III Final, Santiago, Chile.

Zipper, S. C., Jaramillo, F., Wang-Erlandsson, L., Cornell, S. E., Gleeson, T., Porkka, M., … Gordon, L. (2020). Integrating the Water Planetary Boundary With Water Management From Local to Global Scales. Earth's Future, 8(2). https://doi.org/10.1029/2019ef001377

References from Supporting Information

Steiger, R.H., Jager, E., 1977. Subcommission on geochronology: convention on the use of decay constants in geo- and cosmochronology. Earth Planet. Sci. Lett. 36, 359–362.

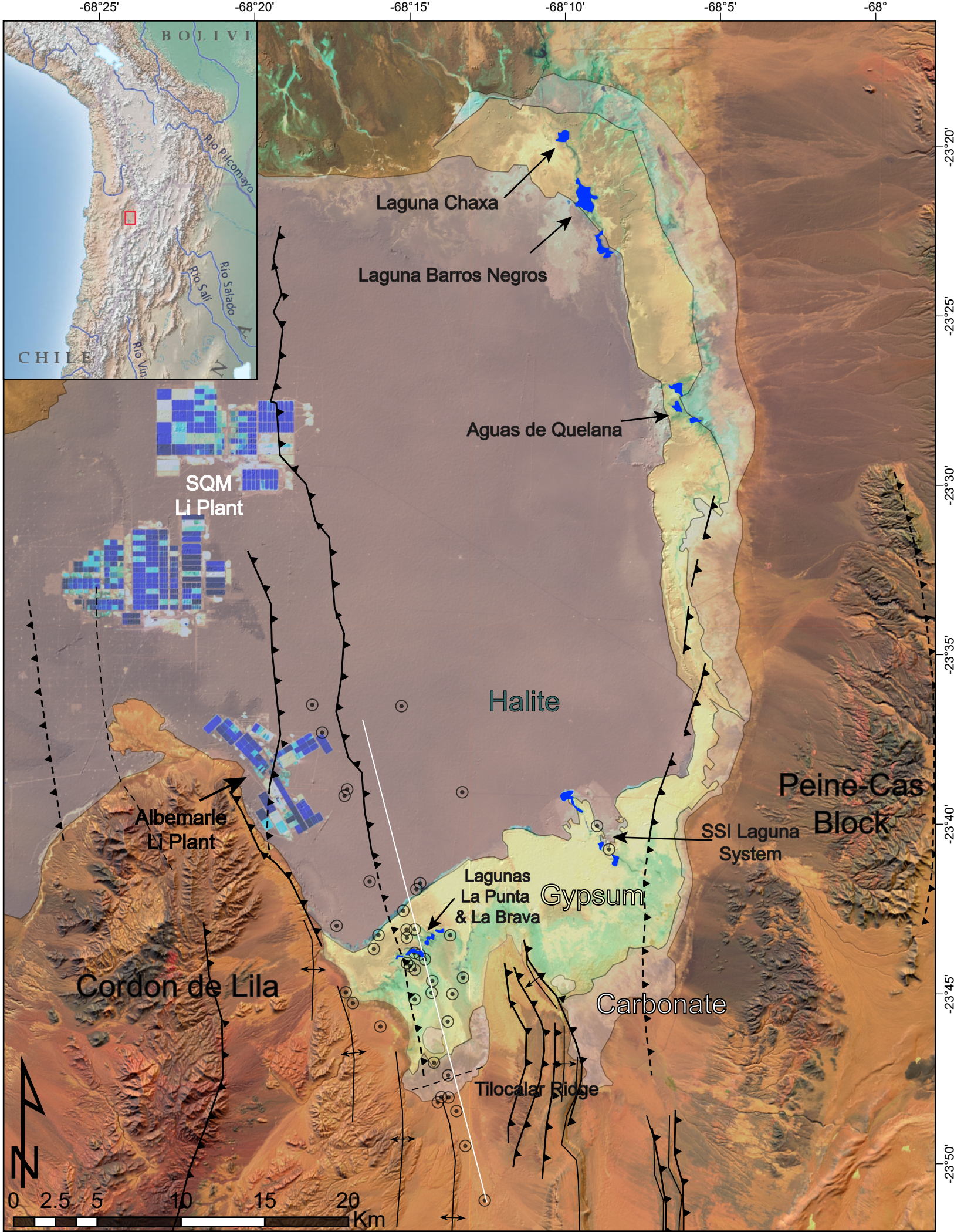
-68°25'
-68°20'
-68°15'
-68°10'
-68°5'
-68°
-23°20'
-23°25'
-23°30'
-23°35'
-23°40'
-23°45'
-23°50'
BOLIVIA
CHILE
Rio Pilcomayo
Rio Salí
Rio Salado
Laguna Chaxa
Laguna Barros Negros
Aguas de Quelana
SQM
Li Plant
Albemarle
Li Plant
Halite
Peine-Cas
Block
SSI Laguna
System
Lagunas
La Punta
& La Brava
Gypsum
Cordon de Lila
Carbonate
Tilocalar Ridge
N
0 2.5 5 10 15 20
Km

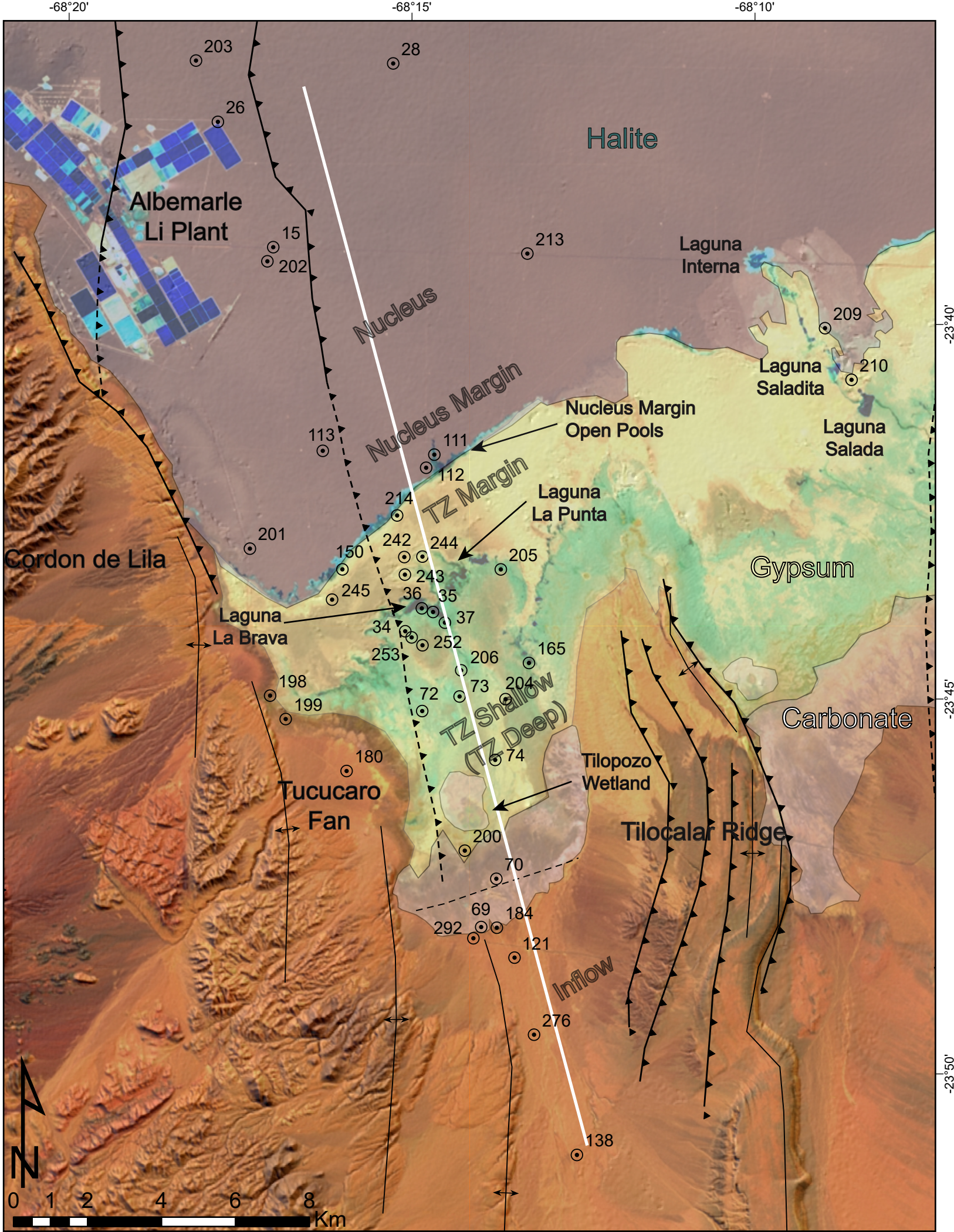
-68°20'
-68°15'
-68°10'
-23°40'
-23°45'
-23°50'
Halite
Albemarle
Li Plant
Nucleus
Nucleus Margin
Laguna
Interna
Laguna
Saladita
Laguna
Salada
Nucleus Margin
Open Pools
TZ Margin
Laguna
La Punta
Gypsum
Cordon de Lila
Laguna
La Brava
Carbonate
TZ Shallow
(TZ Deep)
Tilopozo
Wetland
Tucucaro
Fan
Tilocalar Ridge
Inflow
203
28
26
15
202
213
209
210
113
111
112
214
201
242
244
150
205
243
245
36
35
37
34
252
253
206
165
198
73
204
72
199
74
180
200
70
69
184
292
121
276
138
N
0 1 2 4 6 8
Km

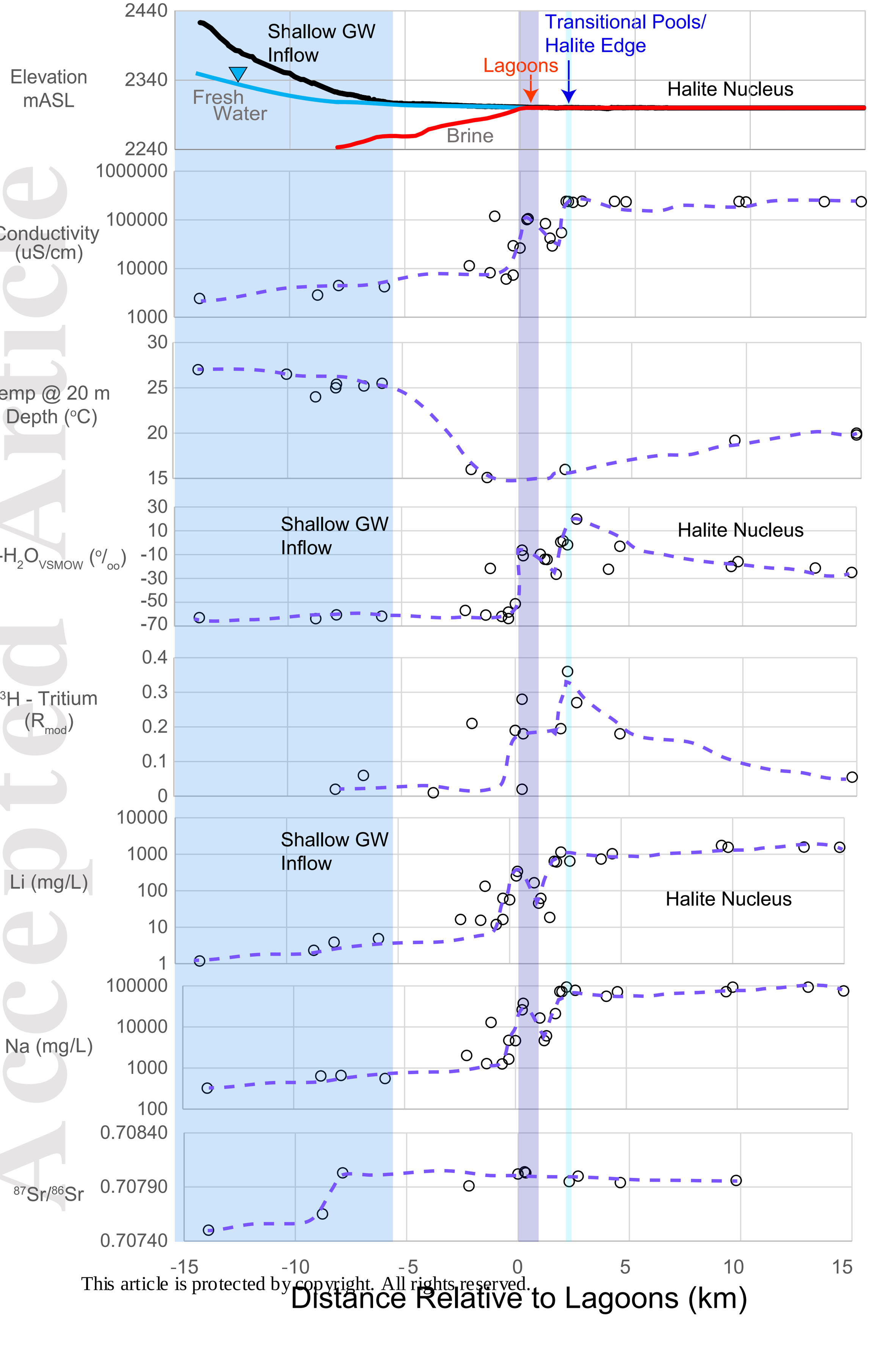

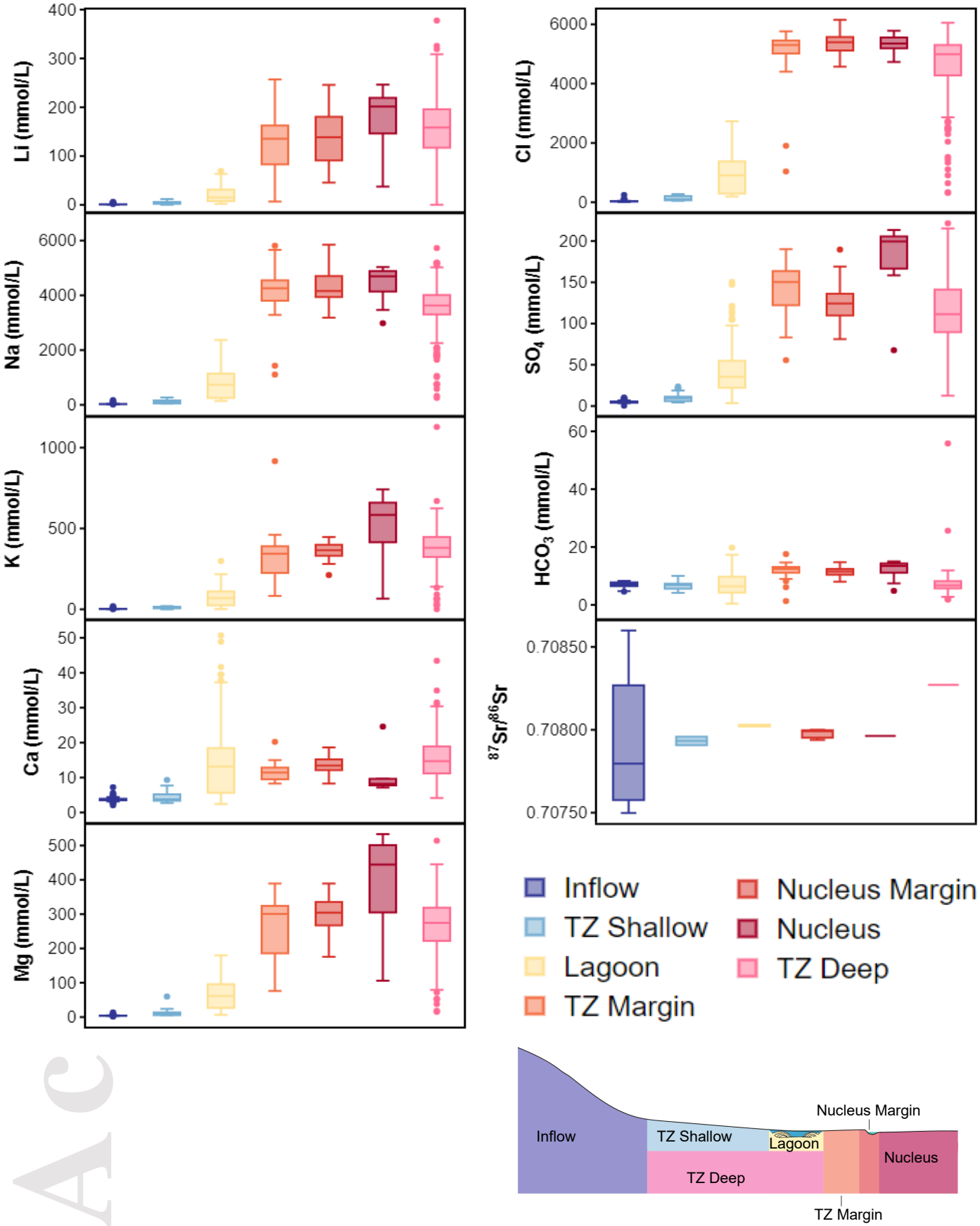

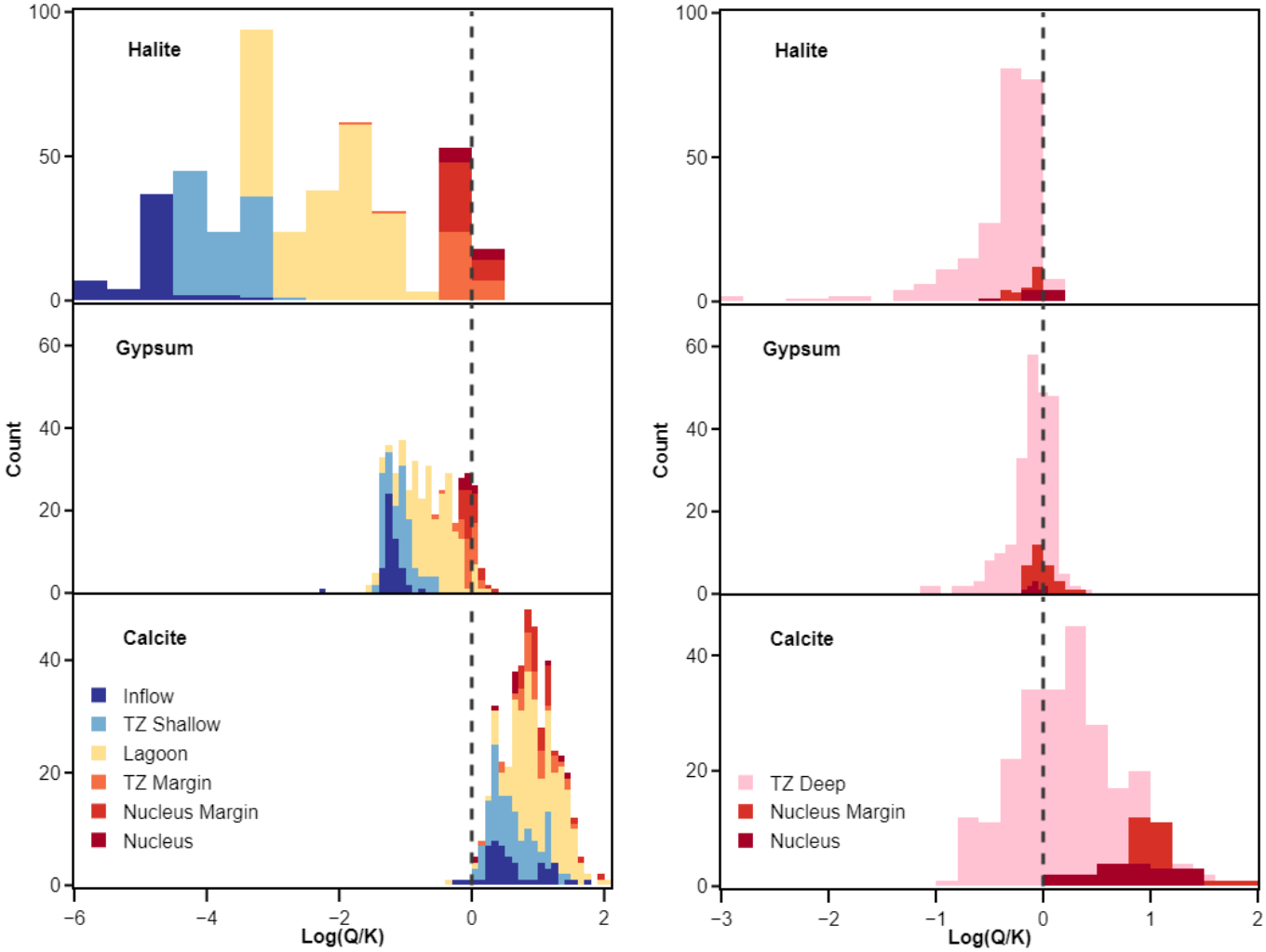

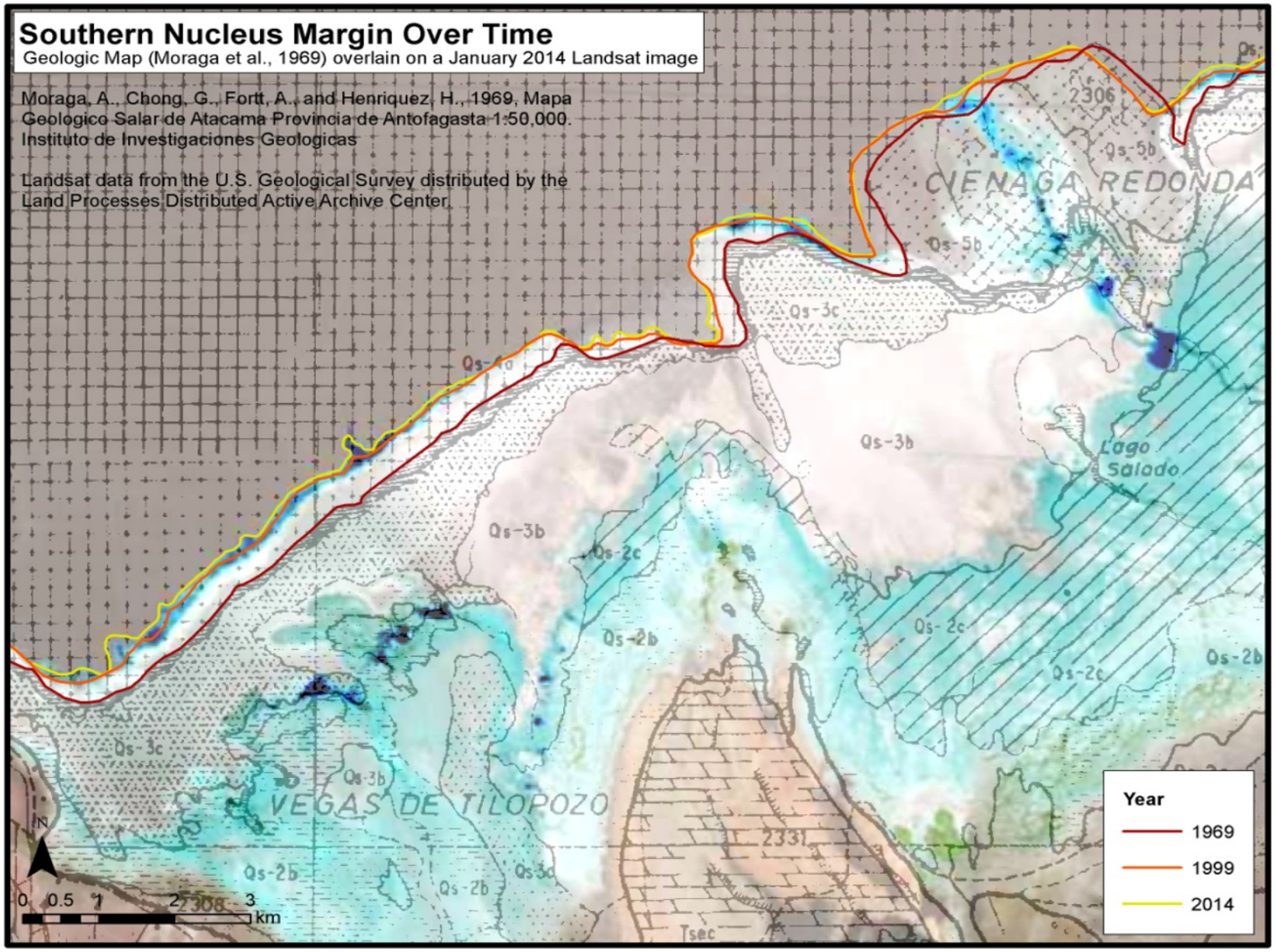

(a)

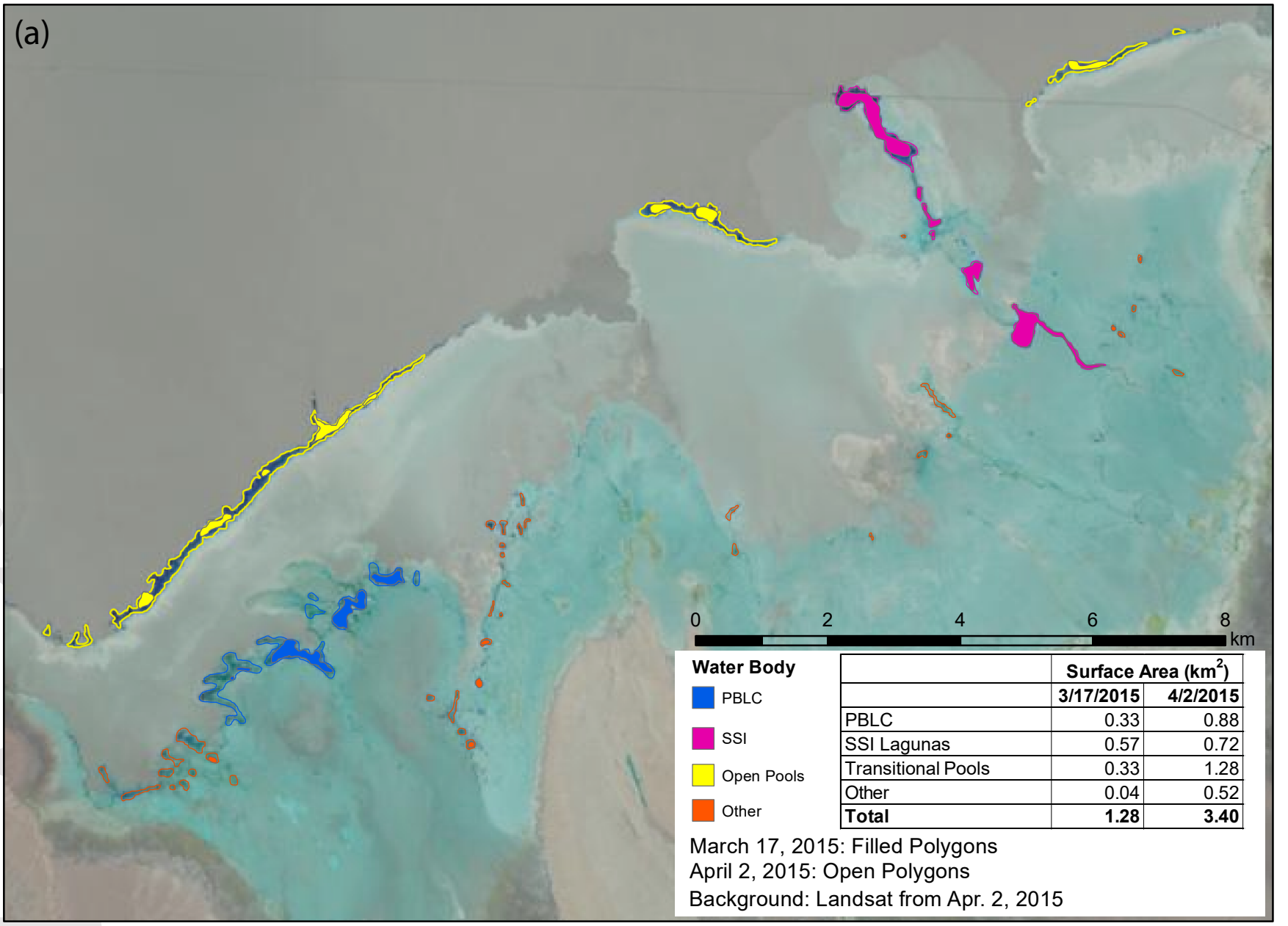

	Surface Area (km^2)	
	3/17/2015	**4/2/2015**
PBLC	0.33	0.88
SSI Lagunas	0.57	0.72
Transitional Pools	0.33	1.28
Other	0.04	0.52
Total	**1.28**	**3.40**

March 17, 2015: Filled Polygons
April 2, 2015: Open Polygons
Background: Landsat from Apr. 2, 2015

(b)

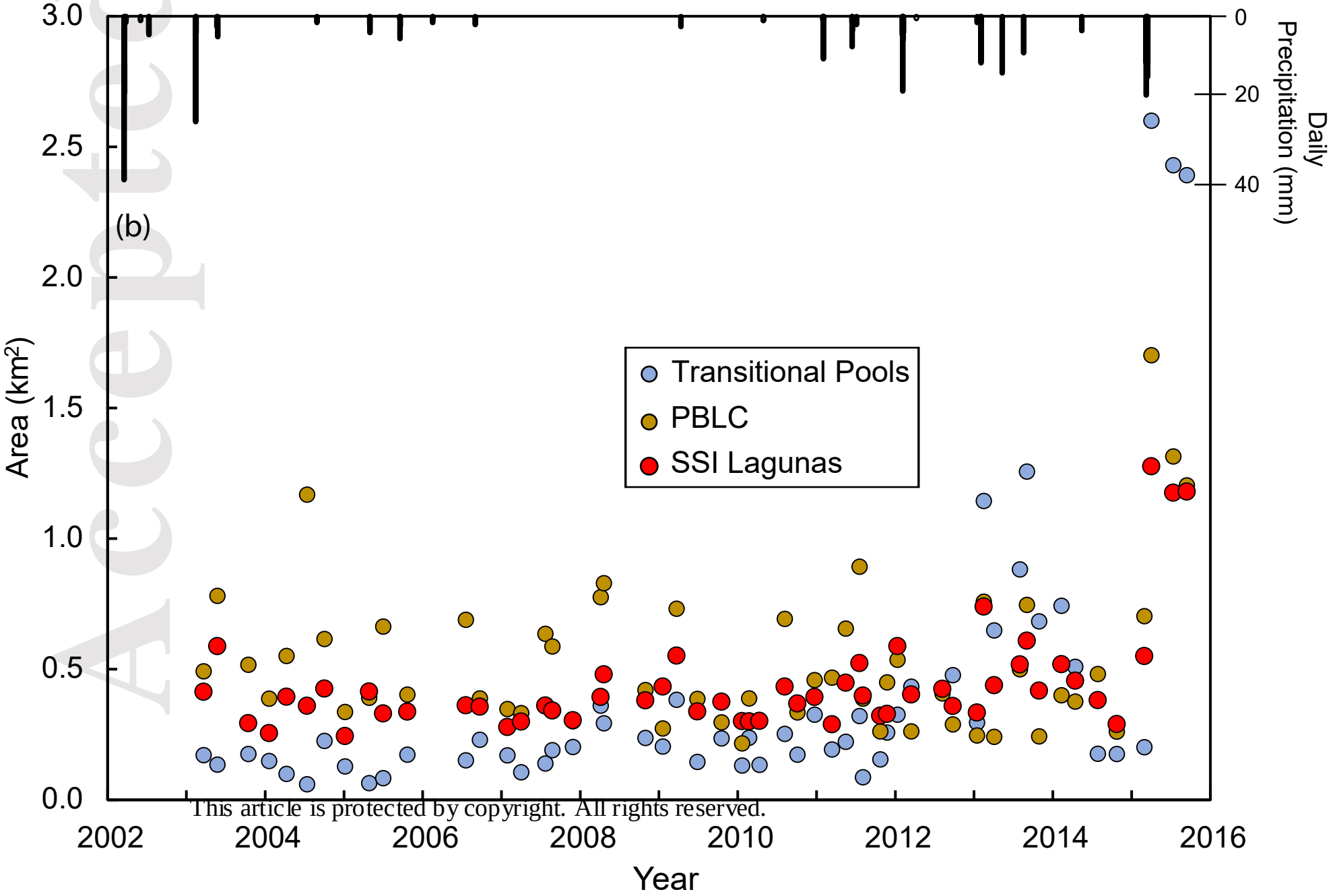

Inflow
Shallow TZ
Lagoons
TZ Margin
Nucleus Margin
Nucleus
Deep TZ

Tufa Mounds
Higher permeability "vuggy" carbonate
Brackish/Brine interface
Re-precipitation of Halite/Gypsum in pore space
Secondary porosity Halite dissolution pathways
1m
Fresh
Brine
30m
100m
200m
15km
Tectonic Subsidence (~0.25m/ka)
Salar Fault System
Caballo Fault
Gypsum Coarse
Gypsum Fine
Halite
Gypsum Medium
5m

Hydrostratigraphic Unit — **Bulk Hydraulic Conductivity (m/d)**

Nucleus Halite	100-1000
Inter-bedded Gypsum & Halite	0.01-100
Carbonate	0.1-100
Alluvium	1-100
Ignimbrite	5-100

Fault
Buried Lagoon Deposit
High Permeability "Vuggy" Carbonate

Fluxes

Evaporation
Precipitation
Fresh Groundwater
Fresh Water
Brackish Water
Brine